Environmental Science & Technology

pubs.acs.org/est

Article

Enhanced Formation of 6PPD-Q during the Aging of Tire Wear Particles in Anaerobic Flooded Soils: The Role of Iron Reduction and Environmentally Persistent Free Radicals

Qiao Xu, Gang Li,* Li Fang, Qian Sun, Ruixia Han, Zhe Zhu, and Yong-Guan Zhu*

Cite This: https://doi.org/10.1021/acs.est.2c08672

Read Online

ACCESS | Metrics & More | Article Recommendations | Supporting Information

ABSTRACT: Rapid urbanization drives increased emission of tire wear particles (TWPs) and the contamination of a transformation product derived from tire antioxidant, termed as *N*-(1,3-dimethylbutyl)-*N*′-phenyl-*p*-phenylenediamine-quinone (6PPD-Q), with adverse implications for terrestrial ecosystems and human health. However, whether and how 6PPD-Q could be formed during the aging of TWPs in soils remains poorly understood. Here, we examine the accumulation and formation mechanisms of 6PPD-Q during the aging of TWPs in soils. Our results showed that biodegradation predominated the fate of 6PPD-Q in soils, whereas anaerobic flooded conditions were conducive to the 6PPD-Q formation and thus resulted in a ∼3.8-fold higher accumulation of 6PPD-Q in flooded soils than wet soils after aging of 60 days. The 6PPD-Q formation in flooded soils was enhanced by Fe reduction-coupled 6PPD oxidation in the first 30 days, while the transformation of TWP-harbored environmentally persistent free radicals (EPFRs) to superoxide radicals ($O_2^{\bullet-}$) under anaerobic flooded conditions further dominated the formation of 6PPD-Q in the next 30 days. This study provides significant insight into understanding the aging behavior of TWPs and highlights an urgent need to assess the ecological risk of 6PPD-Q in soils.

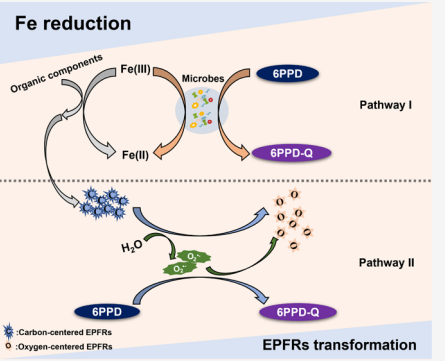

KEYWORDS: *tire wear particles, 6PPD-Q, soil, aging, EPFRs, iron reduction*

INTRODUCTION

Microplastic pollution has been a global environmental issue for decades.[1] Tire wear particles (TWPs) are one of the major types of microplastics in the environment, which account for ∼15% of microplastics in the ocean.[2] Rapid urbanization over the past few decades has resulted in an estimated global average emission rate of 0.81 kg/year per capita of TWPs into the ambient environment,[3] with almost half of these TWPs being transported by non-airborne pathways and eventually entering into soil.[4] However, the potential threat of this emerging pollutant to terrestrial environments is still in its infancy, and research focusing explicitly on TWP-specific properties and processes affecting the fate of TWPs in soil, such as aging, is still lacking.[5]

TWPs consist of rubber, reinforcing agents, vulcanization agents, antioxidants, and so on.[6] Therefore, the environmental risks of TWPs correlate well with these hazardous compounds during the TWP aging processes.[7] Some TWP-specific compounds, such as zinc (Zn) and benzothiazoles (BTs, e.g., benzothiazole (BT) and 2-mercaptobenzothiazole (MBT)), are thus widely used as tire markers to characterize the contamination of TWP globally.[8] However, the specificities of Zn and BTs as tire markers might be restricted due to the interference of other traffic-related sources[9,10] and their easy leachability and instability.[11] Recently, three transformation products of *N*-(1,3-dimethylbutyl)-*N*′-phenyl-*p*-phenylenediamine (6PPD), a globally ubiquitous tire rubber antioxidant, had been identified as promising markers for TWPs in soil.[12] Among them, *N*-(1,3-dimethylbutyl)-*N*′-phenyl-*p*-phenylenediamine-quinone (6PPD-Q) has been suggested as the major causal reason for the acute mortality of coho salmon in urban rivers.[13] The biotoxicity of 6PPD-Q to organisms such as coho salmon (LC_{50} of 95 ng L^{-1})[14] and zebrafish larvae (LC_{50} of 308.67 μg L^{-1})[15] further suggested it as a "very highly toxic" emerging pollutant. Many studies have reported the wide spread of 6PPD-Q in road runoff (with mean concentrations of 80−370 ng L^{-1}),[16] municipal wastewater treatment plant effluents (with a maximum mean mass of 446.5 ± 37.7 ng per Polar Organic Chemical Integrative Sampler (POCIS)),[17] urban dust (median range of 32.2−80.9 ng g^{-1}),[18] $PM_{2.5}$ (annual median concentrations range of 1.7−6.7 pg m^{-3}),[19] and especially, in soils (ranged from 9.50 to 936 ng g^{-1} with an average level of 234 ng g^{-1}).[20] While soil environments are important sinks of TWPs, whether the formation of 6PPD-Q

Received: November 18, 2022
Revised: March 14, 2023
Accepted: March 22, 2023

would be enhanced during the following TWP aging processes in soils is still unclear.

The aging of TWPs in the soil is supposed to be driven by both abiotic and biotic pathways. For example, soil moisture has been identified as an important environmental factor for the aging of pollutants in soils[21] because different water managements might result in anaerobic and aerobic conditions, which further differentiate the transformation of pollutants.[22] Therefore, it can be hypothesized that the aging of TWPs under different water conditions might lead to distinct accumulation of 6PPD-Q in soils. More importantly, aging of microplastics could also promote the formation of environmentally persistent free radicals (EPFRs), a ubiquitous type of free radicals that could remain stable for months and undergo various reactions with water to form reactive oxygen species (ROS),[23] thus influencing key biogeochemical processes on Earth. For instance, EPFRs and ROS were found on microplastics that had been exposed to light, which was thought to promote their formation via chemical chain scission and O_2/H_2O addition,[24] and latest research has found that around 1.0×10^{17} spins/g EPFRs were formed on TWPs during their photoaging processes.[25] Therefore, we hypothesized that the transformation of EPFRs might occur during the TWP aging processes, which further participate in the abiotic oxidation of 6PPD to 6PPD-Q in flooded soils. Additionally, soil microbial communities might facilitate the biotic aging of TWPs in soil when TWPs act as the sole carbon source for some bacteria and fungi.[26] However, the release of antioxidants, commonly reported as 6PPD,[27,28] in the tire may suppress this phenomenon due to their inhibitory effects on bacteria and enzymes.[29] In short, the aging of TWPs in the real soil environment could be mediated by these factors above, whereas the 6PPD-Q formation during TWP aging processes is still poorly understood, hindering the ability to assess the profound impact of TWPs on soil ecosystems.

This study aimed to investigate the dynamic aging of TWPs and the formation of 6PPD-Q under different water conditions in the soil. Therefore, we first examined the accumulation characteristics of 6PPD-Q under different water conditions (wet and flooded) coupled with or without γ-sterilization pretreatment during TWP aging processes in soil. Then, we investigated the linkage between 6PPD-Q accumulation and soil properties and finally identified the key roles of Fe reduction as well as environmentally persistent free radicals (EPFRs) in the 6PPD-Q formation in flooded soils. We further depicted the mechanisms underlying the 6PPD-Q formation under anaerobic flooded conditions during TWP aging processes in soil. The obtained results could expand our understanding of the fate of 6PPD-Q during the TWP aging processes in soil and highlight the potential threat of TWPs to soil health.

MATERIALS AND METHODS

Chemicals. Methanol (99.9%, LC-MS), acetonitrile (99.9%, LC-MS), isopropanol (99.9%, HPLC), 6PPD-quinone (100 μg/mL in acetonitrile), 6PPD-quinone-d_5, coumarin (COU, 99%), 7-hydroxylcoumarin (7-hCOU, 98%), 2,3-bis(2-methoxy-4-nitro-5-sulfophenyl)-2H-tetrazolium-5-carboxanilide (XTT, >90%), L-histidine (LA, 98%), and 2,2-diphenyl-1-picrylhydrazyl (DPPH) were purchased from J&K Scientific, Ltd. (Beijing, China). Cerium(IV) sulfate tetrahydrate ($Ce(SO_4)_2 \cdot 4H_2O$) and nitro blue tetrazolium (NBT, 98%) were purchased from Macklin Biochemical Technology Co., Ltd. (Shanghai, China).

Soil and Tire Wear Particles Sampling. The tested soil was collected from a paddy field located in a periurban area of Zhangxi, Ningbo, Zhejiang Province, China (29°47′32″N, 121°21′47″E), and the characteristics of soil properties are shown in Table S1. Soil samples were air-dried, homogenized, and sieved through 2 mm nylon mesh sieves. Since the TWPs size distribution in a realistic environment was reported to range from the nanosized particle fraction up to 220 μm,[30] the tested TWPs were obtained from a discarded car tire with stainless-steel graters and sieved through a 500 μm mesh according to a previous study with a medium diameter of 225.6 μm before use.[31] The contents of 6PPD and 6PPD-Q in pristine TWPs were determined to be 17.07 ± 4.69 and 135.38 ± 26.88 μg/g, respectively. However, the concentrations of 6PPD and 6PPD-Q in the tested soil were 1.47 ± 0.04 μg/kg and below the detection limit of liquid chromatography with tandem mass spectrometry (LC-MS-MS) (TSQ Vantage triple quadrupole mass spectrometer, equipped with an electrospray ion source (ESI source, Thermo); Ultimate 3000 Ultra High-Performance Liquid Chromatograph (Thermo)), respectively. A demonstration of our experiment design is shown in Figure S1.

Soil Culture Experiment. For the soil culture experiment, the TWPs were homogeneously mixed with 80 g of air-dried soil to obtain a dose of 0.1% (w/w) TWPs in soil. Afterward, it was transferred to a 100 mL glass beaker following the addition of sterilized deionized water. Overall, there were four treatments: (1) NS, nonsterilized soil only; (2) NS_T, nonsterilized soil with TWPs; (3) S, sterilized (a 60 kGy dose of ^{60}Co source before the experiment) soil only; and (4) S_T, sterilized soil and TWPs. Each treatment was divided into two water management regimes: (1) wet conditions, 60% of maximal water holding capacity and (2) flooded conditions, a 3 cm water table above the soil surface. Each group contains three replicates. The culture was conducted in an illumination chamber (196 W) at a 16 h light (25 °C)/8 h dark (20 °C) condition with a relative humidity of 65%. The wavelength ranged from 400 to 800 nm, and the irradiation intensity at 448 nm measured with a radiometer was 0.018 mW cm^{-2}. The same experiments were conducted simultaneously with only one difference, where TWPs were pretransferred into nylon mesh bags (mesh size: 25 μm, height: 8 cm, width: 2 cm) and then buried in soil 2 cm below the surface soil.

At each predetermined time interval (1, 3, 10, 30, and 60 days), soil−TWP mixtures were destructively collected, freeze-dried, and stored at −20 °C for further analysis. The nylon mesh bags containing TWPs were also separated from the soil for further characterization of TWPs.

In addition, we added a series of dark groups with the same culture conditions as flooded treatments without light irradiations (termed dark treatments) to identify the influence of light on ROS formation in the surface water.

Hydroponic Incubation Experiment I. A hydroponic incubation experiment was designed to verify the coupling of Fe reduction to 6PPD oxidation under anaerobic conditions. Briefly, 60 mL of soil solution obtained by extraction of 20 g of air-dried tested soil samples with deionized water was added in a serum bottle, then ferric chloride ($FeCl_3$) and 6PPD were added according to the following setup: (i) Fe(III) + 6PPD + sterilization treatment, with 0.2 g/L Fe^{3+} and 40 μg/L 6PPD in a sterilized soil solution; (ii) 6PPD + sterilization treatment,

https://doi.org/10.1021/acs.est.2c08672
Environ. Sci. Technol. XXXX, XXX, XXX−XXX

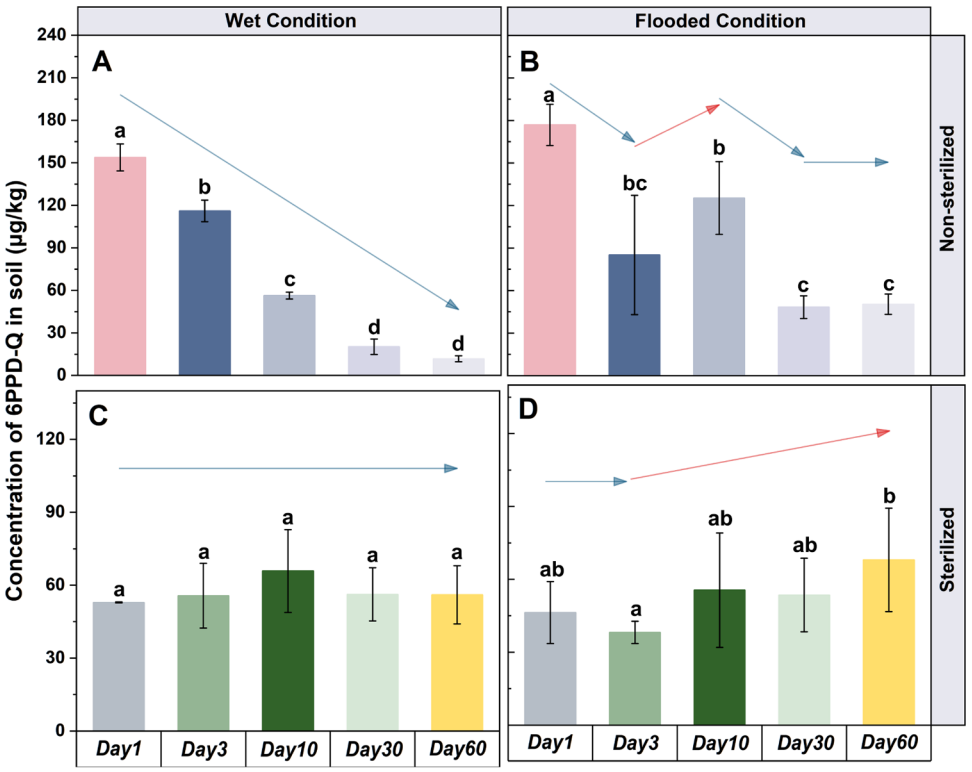

Figure 1. Variations of 6PPD-Q concentration under different conditions ((A, C) 60% WHC condition and (B, D) flooded condition) during TWP aging in soils ((A, B) nonsterilized and (C, D) sterilized with γ-irradiation).

with 40 μg/L 6PPD in a sterilized soil solution; (iii) Fe(III) + 6PPD + nonsterilization treatment, with 0.2 g/L Fe^{3+} and 40 μg/L 6PPD in a nonsterilized soil solution; (iv) 6PPD + nonsterilization treatment, with 40 μg/L 6PPD in nonsterilized soil solution. Each treatment included triplicates and soil solutions were autoclaved at 121 °C for 30 min for sterilization. All serum bottles containing the soil solution were flushed with N_2 and then settled overnight in a glovebox. After that, Fe^{3+} and 6PPD were added and 1 mL of the mixture was withdrawn at each predetermined time interval (0, 1/6, 0.5, 1, 2, 5, 10, 24, 48, and 72 h) to determine Fe(II), 6PPD, and 6PPD-Q.

Hydroponic Incubation Experiment II. Another hydroponic incubation experiment was conducted by homogeneously mixing 50 mg of TWPs with 50 mL of deionized water in each 120 mL brown serum bottle to explore the formation of ROS induced by TWP-harbored EPFRs under flooded conditions and their roles in 6PPD-Q formation. In brief, there were three treatments: (i) TWP groups, with only 0.1% (w/v) TWPs in deionized water; (ii) TWP + NBT groups, with 0.1% (w/v) TWPs and 10 mM NBT in deionized water; and (iii) TWP + LA groups, with 0.1% (w/v) TWPs and 400 mM L-histidine in deionized water. Here, NBT and L-histidine were used as $O_2^{\bullet-}$ and $^{\bullet}OH$ scavengers, respectively.[24,32] Each treatment contained two subgroups: (i) aerobic groups, where serum bottles were incubated under ambient aerobic, dark conditions at room temperature and (ii) anaerobic groups, where all serum bottles were flushed with N_2 to remove the oxygen and then sealed with butyl rubber stoppers, incubated under anaerobic, dark conditions at room temperature. All bottles were placed on an orbital shaker (120 rpm, 25 ± 1 °C) and incubated for 16 days under dark conditions. At each predetermined time interval (0, 1, 3, 7, 12, and 16 days), 1.75 mL of the suspension was withdrawn from each bottle to determine 6PPD-Q and ROS.

Determination of 6PPD, 6PPD-Q, ROS, and Soil Properties. The extraction of 6PPD and 6PPD-Q in soil−TWP mixtures was conducted as reported previously,[12] and the details are presented in Text S1. 1.5 mM COU, 0.05 mM XTT, and 0.5 mM $Ce(SO_4)_2$ were used for the determination of hydroxyl radicals ($^{\bullet}OH$), superoxide ($O_2^{\bullet-}$), and hydrogen peroxide (H_2O_2), respectively.[33−35] Details for the protocols of 7-hCOU, XTT formazan, and Ce $(SO_4)_2$ detection can be found in Text S2−S4. Fe(II) and Fe(III) contents in soil were determined using the 1,10-phenanthroline method,[36] shown in Text S5. The values of soil pH and redox potential (eH) were measured *in situ* using an ion analyzer (Thermo-Orion, Beverly, MA) equipped with a pH electrode and an oxidation reduction potential electrode. Dissolved oxygen (DO) was measured *in situ* using a portable dissolved oxygen electrode (CLEAN DO30, Shanghai ZhenMai Instruments Co., Ltd., China).

FTIR and EPR Analysis. After collection, subsamples of freeze-dried TWPs were used for Fourier transform infrared spectroscopy (FTIR) analysis, and others were placed in an electron paramagnetic resonance (EPR) tube (Wilmad, WG-1000-7, o.d., 5 mm) and determined by an EPR spectrometer (Bruker A300 EPR Spectrometer) at room temperature. The parameters of EPR detection are listed in Text S6. The *g*-factor was determined and calibrated by comparing it with a known standard radical, DPPH,[37] and the radical concentrations were calculated by comparing the signal peak area with DPPH.[38]

Statistical Analysis. Data were presented as mean values ± standard error. Independent-sample *T*-test and one-way ANOVA followed by the Duncan test were performed using IBM SPSS 19.0 (SPSS for Windows, Version 19.0) to identify

https://doi.org/10.1021/acs.est.2c08672
Environ. Sci. Technol. XXXX, XXX, XXX−XXX

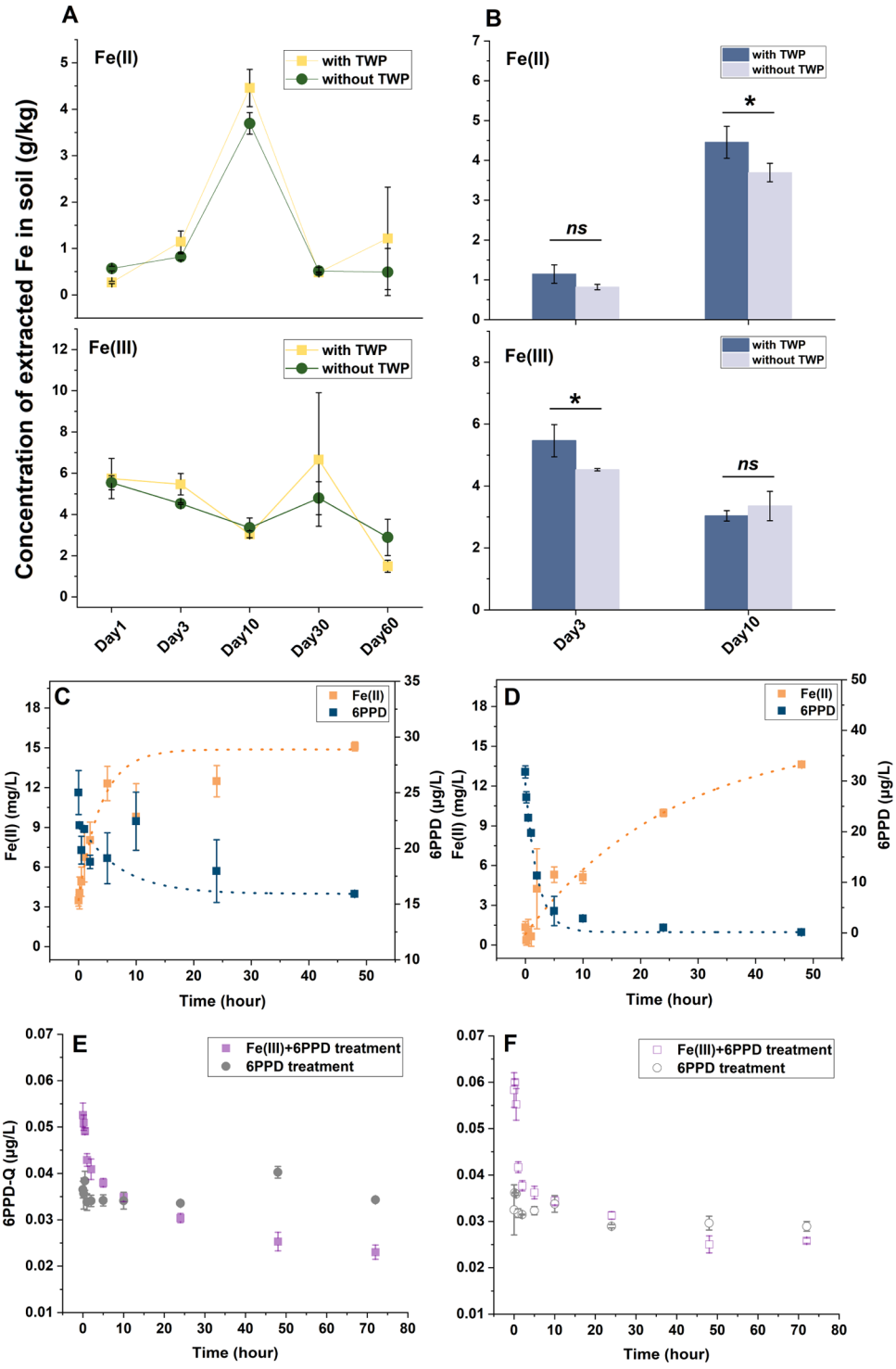

Figure 2. Fe reduction coupling 6PPD degradation under anaerobic conditions. Variation of soil Fe(II) and Fe(III) concentrations during aging processes in nonsterilized soils (A); influence of TWP amendment on the Fe reduction process at the early 10 days (B); dynamics of Fe(II) and 6PPD concentration under nonsterilized (C); and sterilized conditions (D) in hydroponic incubation experiment I; Dynamics of 6PPD-Q concentration under nonsterilized (E) and sterilized conditions (F) in hydroponic incubation experiment I. Significant differences between different conditions (with or without TWPs) are shown as $*p < 0.05$, $**p < 0.01$, and $***p < 0.001$.

the significant difference between different treatments at $p < 0.05$, and data were plotted using Origin2018.

RESULTS AND DISCUSSION

Dynamics of 6PPD and 6PPD-Q Concentrations Under Different Soil Conditions during TWP Aging. A significant and gradual decrease in the 6PPD concentrations was observed in nonsterilized soils (Figure S2A,B), while in sterilized soils only a moderate decrease of 6PPD concentrations under flooded conditions was found (Figure S2C,D). Conversely, the 6PPD-Q concentrations in soil−TWP mixtures varied under different conditions with time (Figure

https://doi.org/10.1021/acs.est.2c08672
Environ. Sci. Technol. XXXX, XXX, XXX−XXX

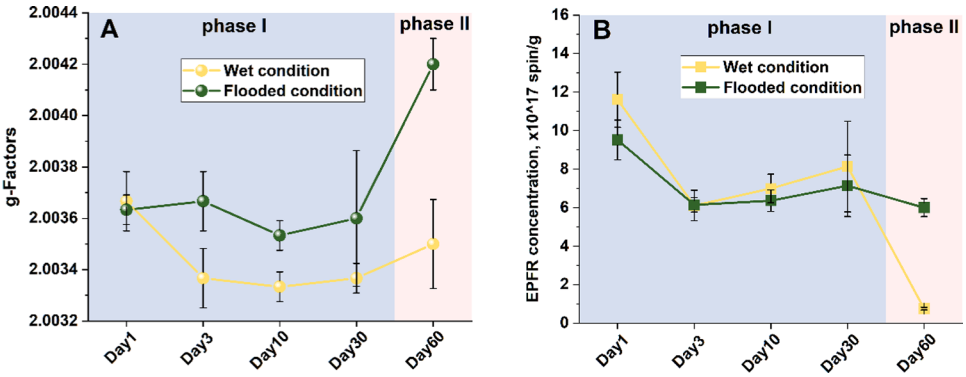

Figure 3. Types (A) and concentrations (B) of EPFRs on TWP samples collected from wet treatments and flooded treatments during the whole aging period.

1). Indeed, the concentration of 6PPD-Q decreased significantly under wet conditions (Figure 1A), whereas in sterilized soils under the same conditions, it remained stable throughout the aging period (Figure 1C), indicating the occurrence and predominance of natural biodegradation of 6PPD-Q[39] under wet conditions. Similar, although persistent, decrease in the concentrations of 6PPD-Q were also found in nonsterilized soils under flooded conditions (Figure 1B). However, it was worth noticing that the decrease of 6PPD-Q concentrations slowed down from day 3 to day 10 under flooded conditions, and 6PPD-Q concentrations on day 10 were even higher than those on day 3, either for sterilized or nonsterilized soil−TWP mixtures (Figure 1B,D). Meanwhile, a modest increase of 6PPD-Q concentrations occurred at the end of the aging period in sterilized soils under the same flooded conditions (Figure 1D).

The variations of 6PPD concentrations in nonsterilized soils were similar under both wet and flooded conditions, indicating similar degradation rates of 6PPD under these two conditions (Figure S2A,B). Significant decreases of 6PPD-Q were identified from day 1 to day 3 (from 176.88 ± 14.53 to 85.10 ± 42.09 μg/kg) and from day 10 to day 30 (from 125.26 ± 25.64 to 48.33 ± 7.99 μg/kg) under flooded conditions (Figure S16B), the latter of which even exhibited a quicker degradation rate of 6PPD-Q than that under wet conditions (from 56.36 ± 2.39 μg/kg on day 10 to 20.25 ± 5.40 μg/kg on day 30) (Figure S16A). Therefore, the delayed decreases of 6PPD-Q concentrations in flooded soils from day 3 to day 10 were probably due to the replenishment of newly formed 6PPD-Q, or, the enhanced formation of 6PPD-Q during this stage.

Coupling of Fe Reduction to 6PPD-Q Formation in Anaerobic Flooded Soils. The dissolved oxygen levels in soil−TWP mixtures under flooded conditions during the whole culture period were lower than 0.5 mg/L (Figures S3 and S4), suggesting anaerobic conditions in flooded soils. Our findings indicated that anaerobic flooded conditions facilitated the oxidation of 6PPD to 6PPD-Q during TWP aging in soils, as Tian et al. also confirmed that the oxidation of 6PPD formed 6PPD-Q.[14] As reported previously, long-term anoxia accelerated the accumulation of Fe(II) in soil through microbial reduction of iron hydroxide, which could further couple the degradation of pollutants.[36,40] Herein, a gradual rise of the Fe(II) concentrations to a peak level on day 10 and a decrease to a low level during the subsequent period were observed (Figure 2A), which is consistent with the peak value of the relative abundance (RA) in most typical Fe reducing bacteria[41] on day 10 (Figure S7A). Notably, from day 3 to day 10 after TWP amendment, a synchronous decrease in Fe(III) and an increase in Fe(II) was observed (Figure 2B), correlating well with the decrease of 6PPD (Figure S2B) and the maintenance of 6PPD-Q at this stage (Figure 1B), and the RA in *Bacillus*, the most abundant Fe reducing bacteria in tested soil, was increased with TWP amendment (Figure S7B). However, such Fe reduction at this stage was not observed in sterilized flooded soils (Figure S5). Therefore, our first hypothesis was that the oxidation of 6PPD in the soil−TWP mixture might have been coupled to microbial Fe reduction during the aging processes, thus leading to the formation of 6PPD-Q in flooded soil.

We further conducted the hydroponic incubation experiment I to explore the Fe reduction-coupled 6PPD oxidation under anaerobic conditions. A significant coupling of Fe(II) accumulation to 6PPD degradation was observed in nonsterilized treatments (Figure 2C) rather than sterilized treatments (Figure 2D). Soil solution was settled overnight in the glovebox before Fe^{3+} and 6PPD addition during which more initial substrate would be consumed by microbes in nonsterilized treatments than in sterilized treatments. The following addition of 6PPD could provide the substrate for the microbial Fe reduction process, thus leading to a good coupling of Fe reduction to 6PPD degradation in nonsterilized treatments (Figure 2C). However, in sterilized treatments, the redox-active components in soil solution, such as dissolved organic matter (DOM), might act as electron shuttle,[42] thus leading to separate Fe reduction and 6PPD degradation (Figure 2D). The higher 6PPD-Q concentration in Fe(III) + 6PPD treatments than 6PPD treatments at the early stage further confirmed the key role of microbial Fe reduction in the oxidation of 6PPD to 6PPD-Q, which also facilitated the following degradation of 6PPD-Q (Figure 2E). The higher 6PPD-Q concentration in sterilized soil solution with Fe(III) amendment at the early stage (Figure 2F) might be due to the excess of Fe(III) addition considering that the degradation of 6PPD in Fe(III) + 6PPD treatment was complete in 10 min. Therefore, the microbial Fe reduction coupling with 6PPD-Q formation process could be a plausible pathway for the biotic 6PPD-Q formation during the early stage of TWP aging in flooded soils.

Transformation of Environmentally Persistent Free Radicals during TWP Aging. In addition to the microbial Fe-dependent pathway above, an abiotic 6PPD-Q formation under anaerobic flooded conditions was also confirmed by the increased 6PPD-Q concentrations in sterilized flooded soils

https://doi.org/10.1021/acs.est.2c08672
Environ. Sci. Technol. XXXX, XXX, XXX−XXX

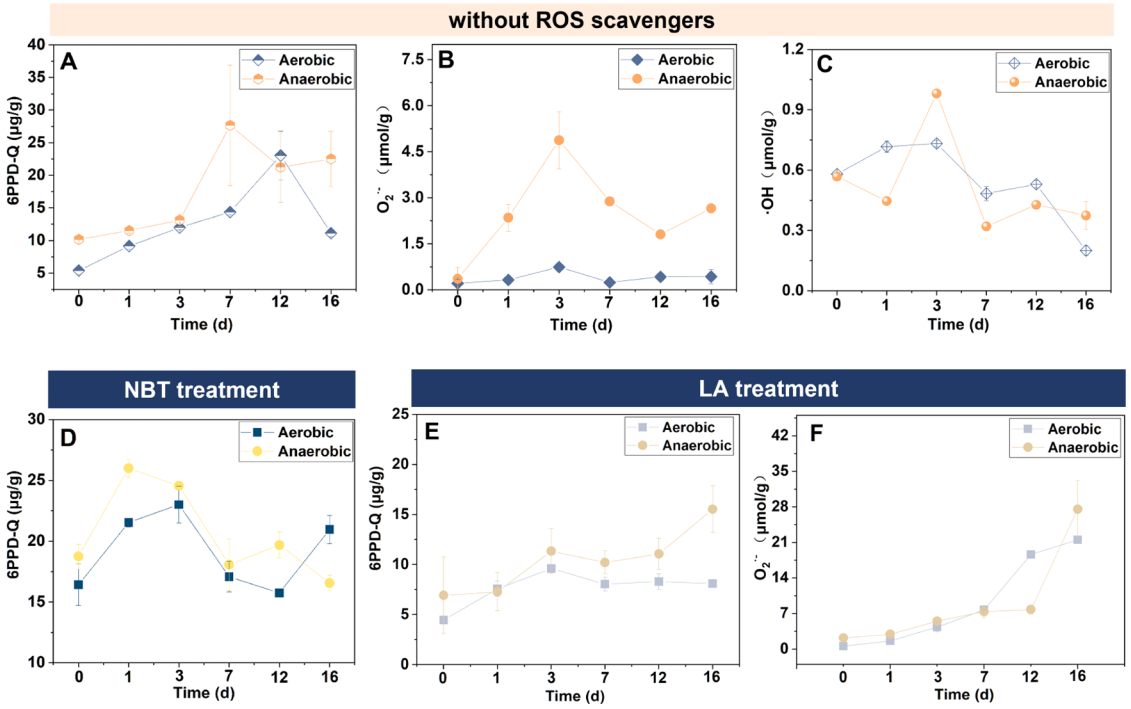

Figure 4. Dynamics of 6PPD-Q (A), $^{\bullet}$OH (B), and $O_2^{\bullet-}$ (C) concentrations in hydroponic incubation experiment II, and their variations with NBT treated as $O_2^{\bullet-}$ scavenger (D) or LA treated as $^{\bullet}$OH scavenger (E, F).

(Figure 1D). Since the influence of light-induced formation of ROS in the upper surface water on 6PPD-Q formation was excluded (Text S8 and Figures S8−S11), the transformation of TWP-harbored EPFRs and their role in the abiotic formation of 6PPD-Q was not clear. Therefore, another series of TWPs were put into nylon mesh bags and aged under the same soil experimental conditions to better understand the effects of aging on TWP-harbored EPFR transformation. The aging degree of TWPs in different treatments was analyzed by FTIR. Five major characteristic peaks at 3600−3700, ∼3100, ∼1700, 1446, and 940−1130 cm^{-1} were observed (Figure S12), which can be ascribed to O−H stretching of carboxyl and hydroxyl groups, N−H stretching vibration, the characteristic peak intensity of quinoid C═O, C−H deformation for methyl and methylene groups, and C−O groups, respectively.[43−45] High signal intensities of these distinct groups were found in flooded treatments compared to wet treatments after the aging of TWPs (Figure S12A). Specifically, the peaks of O−H stretching of carboxyl, hydroxyl, and C−O groups increased over time in flooded treatments, while they decreased remarkably in wet treatments (Figure S12B). All of these results suggested enhanced aging of TWPs under flooded conditions.

The differences in EPFR types and concentrations across time and TWP sample types were further detected by EPR (Figure 3). Generally, EPFRs are common in organically contaminated soils[46] and could be classified into three types according to their *g*-factor values, including carbon-centered radical species (*g*-factor < 2.0030), carbon-centered radicals with a nearby heteroatom, such as oxygen or halogen (2.0030 < *g*-factor < 2.0040), and oxygen-centered radicals (*g*-factor > 2.0040).[47,48] Over time, the majority of EPFRs in wet treatments were mainly carbon-centered radicals with a nearby heteroatom (2.0032 < *g*-factors < 2.0038) (Figure 3A), while EPFRs in flooded treatments were carbon-centered (*g*-factors < 2.0038) during the first 30 days of aging (Figure 3A, phase I) and were oxygen-centered (*g*-factor > 2.0040) in the next 30 days (Figure 3A, phase II). Meanwhile, the concentrations of EPFRs decreased from ∼9×10^{17} to ∼6×10^{17} spin/g after the first 3 days for both wet and flooded treatments and remained stable during the first 30 days (Figure 3B, phase I). A single-electron transfer between transition metals (e.g., Fe(III)) and aromatic molecules, as well as the breaking of the covalent bond, have been reported as major mechanisms for forming EPFRs.[49] This correlated well with the increased Fe (III) reduction with TWPs under flooded conditions (Figure 2A), and the decreased peaks of O−H and C−O groups in TWPs under wet conditions at this stage (Figure S12B), thereby leading to the differentiation of *g*-factors of EPFRs between flooded and wet treatments (Figure 3A, phase I). Afterward, a significant decrease in EPFR concentrations in wet treatment was observed in the next 30 days (Figure 3B, phase II), indicating the consumption of EPFRs in wet soils. Interestingly, the concentrations of EPFRs in flooded treatments maintained stable but with a significant increase of *g*-factors from ∼2.0036 to ∼2.0042 in the next 30 days (Figure 3, phase II), and a smooth decrease and significant accumulation of 6PPD-Q during this stage were also found in nonsterilized and sterilized flooded soils, respectively (Figure 1B,D). The maintenance of carbon-centered EPFRs in flooded treatments during the first 30 days might be due to the contribution of organic components in TWPs (e.g., polycyclic aromatic hydrocarbons (PAHs))[31] and Fe to generating EPFRs considering the similar g-factor of EPFRs in flooded treatments (∼2.0036) to that generated in PAHs contaminated soil.[38] Such an interaction was weakened with the content of total extracted Fe decreased in the next 30 days (Figure S6), thus leading to the differentiation of *g*-factors in the next 30 days. The *g*-factor of ∼2.0042 was also a characteristic of oxygen-centered EPFRs, namely, semiquinone-type EPFRs,[50] which

https://doi.org/10.1021/acs.est.2c08672
Environ. Sci. Technol. XXXX, XXX, XXX−XXX

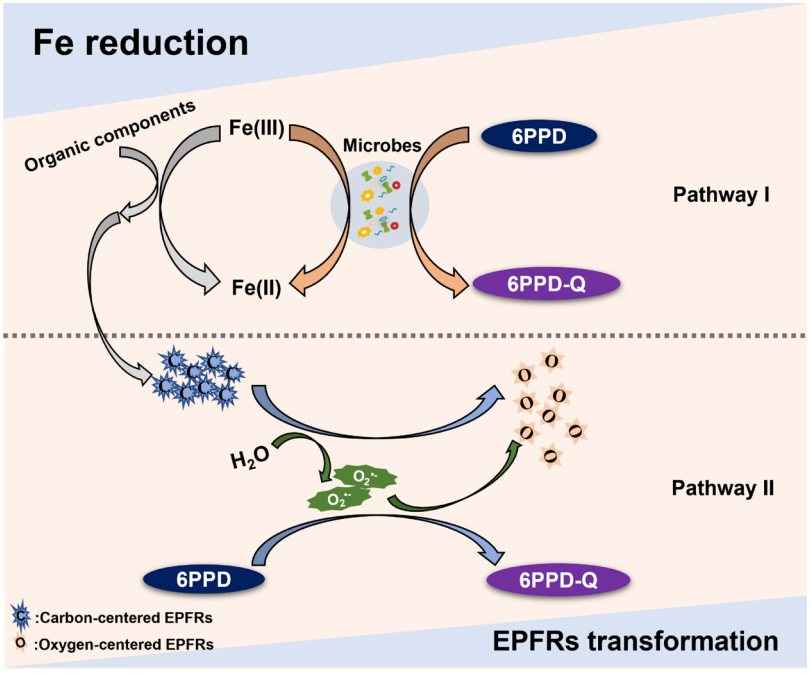

Figure 5. Scheme of proposed pathways for the 6PPD-Q formation under anaerobic flooded conditions during TWP aging in soils.

might be important redox-active moieties for the transformation of 6PPD to 6PPD-Q based on their molecular structure.[39] Therefore, we hypothesized that the reaction of these carbon-centered EPFRs with water might produce ROS, which further contribute to the generation of oxygen-centered EPFRs and following abiotic 6PPD-Q formation under anaerobic flooded conditions.

Environmentally Persistent Free-Radical-Induced Formation of 6PPD-Q. Hydroponic incubation experiment II was conducted to understand the role of EPFR-induced ROS on the abiotic formation of 6PPD-Q under anaerobic flooded conditions. Our results demonstrated that more 6PPD-Q were formed under anaerobic conditions than aerobic conditions (Figure 4A). A higher accumulation of $O_2^{\bullet-}$ was also observed under anaerobic conditions than aerobic conditions (Figure 4B), which correlated well with the increase of 6PPD-Q under anaerobic conditions. Moreover, the increase of 6PPD-Q was inhibited with NBT treatments (Figure 4D). However, it was less affected by LA treatments (Figure 4E). Both $^{\bullet}OH$ and $O_2^{\bullet-}$ were undetectable in NBT treatments, while an increased $O_2^{\bullet-}$ was observed in LA treatments (Figure 4E), and the enhanced correlation between 6PPD-Q and $O_2^{\bullet-}$ under anaerobic conditions compared to aerobic conditions (Figure S13) further consolidated the important role of $O_2^{\bullet-}$ on the 6PPD-Q formation, while $^{\bullet}OH$ probably facilitated the degradation of 6PPD-Q under anaerobic conditions (Figure S14B). Therefore, the formation of $O_2^{\bullet-}$ induced by EPFRs could be a possible pathway for the abiotic 6PPD-Q formation under anaerobic flooded conditions.

Mechanisms for the 6PPD-Q Formation during TWP Aging in Flooded Soils. The results demonstrated that an enhanced formation of 6PPD-Q occurred under anaerobic flooded conditions during TWP aging processes (Figure 1). The Fe reduction as well as EPFR-induced $O_2^{\bullet-}$ formation would likely contribute to the biotic and abiotic 6PPD-Q formation by the proposed pathways as follow (Figure 5): (I) At the beginning of aging, the microbial Fe(III) reduction to Fe(II) was enhanced with time (Figure 2A), which then facilitated the oxidation of 6PPD (Figure 2B,C) and thus predominated the biotic formation of 6PPD-Q during this stage (from day 3 to day 10) (Figures 1B and S7). Meanwhile, the Fe reduction-coupled transformation of multiorganic components in TWPs was also conducive to the formation of carbon-centered EPFRs and helped maintain the EPFR concentrations at a stable level in the first 30 days (Figure 3B); (II) In the next 30 days, the microbial Fe reduction was weakened (Figures 2A and S7A), while the transformation of EPFRs induced by H_2O molecules was predominant (Figure 3A), leading to the formation of ROS (mainly $O_2^{\bullet-}$) (Figure 4B). Then, the active $O_2^{\bullet-}$ directly promoted the abiotic oxidation of 6PPD (Figure 4) to form the redox-active moieties, termed as semiquinone-type EPFRs (Figure 3), and further to 6PPD-Q (Figures 1B,D and S15).

Environmental Implications. This study investigated the dynamic accumulations of 6PPD-Q during TWP aging in soils under different circumstances. Our results showed that biodegradation predominated the fate of 6PPD-Q in soils, whereas flooded conditions were conducive to the 6PPD-Q formation and therefore resulted in a higher accumulation of 6PPD-Q in soils than wet conditions after aging of 60 days. Such accumulation of 6PPD-Q will increase the exposure risk of plants, animals, and even human beings through soils, especially for urban greenbelt soils. The oxidation of 6PPD to 6PPD-Q under anaerobic flooded conditions was proposed to be facilitated by microbial Fe reduction in the first 30 days and EPFR-induced formation of ROS (mainly $O_2^{\bullet-}$) in the next 30 days, which could provide a plausible explanation for the occurrence of 6PPD-Q in anaerobic environments, such as flooded soils, sediments, and natural waters. It would be helpful to expand our understanding of the potential risk of TWPs to soil health. This study also emphasizes the importance of focusing on the role of TWP-harbored EPFRs in controlling the redox processes in the environment. Since

https://doi.org/10.1021/acs.est.2c08672
Environ. Sci. Technol. XXXX, XXX, XXX−XXX

the TWP-harbored EPFRs could promote the oxidation of 6PPD in relatively anaerobic conditions, it might also profoundly influence the way of many biogeochemical processes such as anaerobic ammonium oxidation and Fe redox as well as contaminants transformation in soil ecosystems. Therefore, further studies on the biogeochemical behaviors of TWPs are urgently needed.

■ ASSOCIATED CONTENT

Supporting Information

The Supporting Information is available free of charge at https://pubs.acs.org/doi/10.1021/acs.est.2c08672.

Extraction protocols for 6PPD and 6PPD-Q; determination parameters for LC-MS-MS and EPR; details on the determination and quantification of ROS; physicochemical properties of soil samples; FTIR spectrum of TWP in different treatments; bacterial 16S rRNA gene amplification, sequencing, and bioinformatic analysis; and influence of the light-induced formation of ROS on 6PPD-Q formation (PDF)

■ AUTHOR INFORMATION

Corresponding Authors

Gang Li − *Key Laboratory of Urban Environment and Health, Ningbo Urban Environment Observation and Research Station, Institute of Urban Environment, Chinese Academy of Sciences, Xiamen 361021, P. R. China; Zhejiang Key Laboratory of Urban Environmental Processes and Pollution Control, CAS Haixi Industrial Technology Innovation Center in Beilun, Ningbo 315830, P. R. China;* orcid.org/0000-0002-1674-4587; Email: gli@iue.ac.cn

Yong-Guan Zhu − *Key Laboratory of Urban Environment and Health, Ningbo Urban Environment Observation and Research Station, Institute of Urban Environment, Chinese Academy of Sciences, Xiamen 361021, P. R. China; Zhejiang Key Laboratory of Urban Environmental Processes and Pollution Control, CAS Haixi Industrial Technology Innovation Center in Beilun, Ningbo 315830, P. R. China;* orcid.org/0000-0003-3861-8482; Email: ygzhu@rcees.ac.cn

Authors

Qiao Xu − *Key Laboratory of Urban Environment and Health, Ningbo Urban Environment Observation and Research Station, Institute of Urban Environment, Chinese Academy of Sciences, Xiamen 361021, P. R. China; Zhejiang Key Laboratory of Urban Environmental Processes and Pollution Control, CAS Haixi Industrial Technology Innovation Center in Beilun, Ningbo 315830, P. R. China*

Li Fang − *Key Laboratory of Health Risk Factors for Seafood of Zhejiang Province, Zhoushan Municipal District Center for Disease Control and Prevention, Zhoushan 316000, P. R. China*

Qian Sun − *CAS Key Laboratory of Urban Pollutant Conversion, Institute of Urban Environment, Chinese Academy of Sciences, Xiamen 361021, P. R. China;* orcid.org/0000-0002-0774-1608

Ruixia Han − *Key Laboratory of Urban Environment and Health, Ningbo Urban Environment Observation and Research Station, Institute of Urban Environment, Chinese Academy of Sciences, Xiamen 361021, P. R. China; Zhejiang Key Laboratory of Urban Environmental Processes and Pollution Control, CAS Haixi Industrial Technology Innovation Center in Beilun, Ningbo 315830, P. R. China*

Zhe Zhu − *Department of Chemical and Environmental Engineering, Faculty of Science and Engineering, University of Nottingham, Ningbo 315100, P. R. China*

Complete contact information is available at: https://pubs.acs.org/10.1021/acs.est.2c08672

Notes

The authors declare no competing financial interest.

■ ACKNOWLEDGMENTS

This work was supported by the National Natural Science Foundation of China (42207010 and 42021005).

■ REFERENCES

(1) Koelmans, A. A.; Redondo-Hasselerharm, P. E.; Nor, N. H. M.; Ruijter, V. N. D.; Mintenig, S. M.; Kooi, M. Risk assessment of microplastic particles. *Nat. Rev. Mater.* **2022**, *7*, 138−152.

(2) Schmidt, C.; Krauth, T.; Wagner, S. Export of plastic debris by rivers into the sea. *Environ. Sci. Technol.* **2017**, *52*, 927.

(3) Kole, P. J.; Lohr, A. J.; Van Belleghem, F. G. A. J.; Ragas, A. M. J. Wear and tear of tyres: A stealthy source of microplastics in the environment. *Int. J. Environ. Res. Public Health* **2017**, *14*, 1265.

(4) Knight, L. J.; Parker-Jurd, F. N. F.; Al-Sid-Cheikh, M.; Thompson, R. C. Tyre wear particles: An abundant yet widely unreported microplastic? *Environ. Sci. Pollut. Res.* **2020**, *27*, 18345−18354.

(5) Ding, J.; Lv, M.; Zhu, D.; Leifheit, E. F.; Chen, Q. L.; Wang, Y. Q.; Chen, L. X.; Rillig, M. C.; Zhu, Y. G. Tire wear particles: An emerging threat to soil health. *Crit. Rev. Environ. Sci. Technol.* **2023**, *53*, 239−257.

(6) Halle, L. L.; Palmqvist, A.; Kampmann, K.; Khan, F. R. Ecotoxicology of micronized tire rubber: past, present and future considerations. *Sci. Total Environ.* **2020**, *706*, No. 135694.

(7) McIntyre, J. K.; Prat, J.; Cameron, J.; Wetzel, J.; Mudrock, E.; Peter, K. T.; Tian, Z. Y.; Mackenzie, C.; Lundin, J.; Stark, J. D.; King, K.; Davis, J. W.; Kolodziej, E. P.; Scholz, N. L. Treading water: Tire wear particle leachate recreates an urban runoff mortality syndrome in coho but not chum salmon. *Environ. Sci. Technol.* **2021**, *55*, 11767−11774.

(8) Wik, A.; Dave, G. Occurrence and effects of tire wear particles in the environment - A critical review and an initial risk assessment. *Environ. Pollut.* **2009**, *157*, 1−11.

(9) Fauser, P.; Tjell, J. C.; Mosbaek, H.; Pileegard, K. Quantification of tire-tread particles using extractable organic zinc as tracer. *Rubber Chem. Technol.* **1999**, *72*, 969−977.

(10) Rhodes, E. P.; Ren, Z.; Mays, D. C. Zinc leaching from tire crumb rubber. *Environ. Sci. Technol.* **2012**, *46*, 12856−12863.

(11) Ni, H. G.; Lu, F. H.; Luo, X. L.; Tian, H. Y.; Zeng, E. Y. Occurrence, phase distribution, and mass loadings of benzothiazoles in riverine runoff of the Pearl River Delta, China. *Environ. Sci. Technol.* **2008**, *42*, 1892−1897.

(12) Klöckner, P.; Seiwert, B.; Wagner, S.; Reemtsma, T. Organic markers of tire and road wear particles in sediments and soils: Transformation products of major antiozonants as promising candidates. *Environ. Sci. Technol.* **2021**, *55*, 11723−11732.

(13) Tian, Z. Y.; Zhao, H. Q.; Peter, K. T.; Gonzalez, M.; Wetzel, J.; Wu, C.; Hu, X. M.; Prat, J.; Mudrock, E.; Hettinger, R.; Cortina, A. E.; Biswas, R. G.; Kock, F. V. C.; Soong, R.; Jenne, A.; Du, B. W.; Hou, F.; He, H.; Lundeen, R.; Gilbreath, A.; Sutton, R.; Scholz, N. L.; Davis, J. W.; Dodd, M. C.; Simpson, A.; McIntyre, J. K.; Kolodziej, E. P. A ubiquitous tire rubber-derived chemical induces acute mortality in coho salmon. *Science* **2021**, *371*, 185−189.

(14) Tian, Z. Y.; Gonzalez, M.; Rideout, C. A.; Zhao, H. N.; Hu, X. M.; Wetzel, J.; Mudrock, E.; James, C. A.; McIntyre, J. K.; Kolodziej, E. P. 6PPD-quinone: Revised toxicity assessment and quantification

with a commercial standard. *Environ. Sci. Technol. Lett.* **2022**, *9*, 140−146.
(15) Varshney, S.; Gora, A. H.; Siriyappagouder, P.; Kiron, V.; Olsvik, P. A. Toxicological effects of 6PPD and 6PPD quinone in zebrafish larvae. *J. Hazard. Mater.* **2021**, *424*, No. 127623.
(16) Challis, J. K.; Popick, H.; Prajapati, S.; Harder, P.; Giesy, J. P.; McPhedran, K.; Brinkmann, M. Occurrences of tire rubber-derived contaminants in cold-climate urban runoff. *Environ. Sci. Technol. Lett.* **2021**, *8*, 961−967.
(17) Johannessen, C.; Metcalfe, C. D. The occurrence of tire wear compounds and their transformation products in municipal wastewater and drinking water treatment plants. *Environ. Monit. Assess.* **2022**, *194*, 10.
(18) Huang, W.; Shi, Y. M.; Huang, J. L.; Deng, C. L.; Tang, S. Q.; Liu, X. T.; Chen, D. Occurrence of substituted *p*-phenylenediamine antioxidants in dusts. *Environ. Sci. Technol. Lett.* **2021**, *8*, 381−385.
(19) Zhang, Y. H.; Xu, C. H.; Zhang, W. F.; Qi, Z. H.; Song, Y. Y.; Zhu, L.; Dong, C.; Chen, J. M.; Cai, Z. W. *p*-Phenylenediamine antioxidants in $PM_{2.5}$: The underestimated urban air pollutants. *Environ. Sci. Technol.* **2022**, *56*, 6914−6921.
(20) Cao, G. D.; Wang, W.; Zhang, J.; Wu, P. F.; Zhao, X. C.; Yang, Z.; Hu, D.; Cai, Z. W. New evidence of rubber-derived quinones in water, air, and soil. *Environ. Sci. Technol.* **2022**, *56*, 4142−4150.
(21) Xu, Q.; Ye, B. H.; Mou, X. Y.; Ye, J. E.; Liu, W. Y.; Luo, Y. T.; Shi, J. Y. Lead was mobilized in acid silty clay loam paddy soil with potassium dihydrogen phosphate (KDP) amendment. *Environ. Pollut.* **2019**, *255*, No. 113179.
(22) Xie, W. J.; Zhang, P.; Liao, W. J.; Tong, M.; Yuan, S. H. Ligand-enhanced electron utilization for trichloroethylene degradation by $^{\bullet}OH$ during sediment oxygenation. *Environ. Sci. Technol.* **2021**, *55*, 7044−7051.
(23) Sigmund, G.; Santin, C.; Pignitter, M.; Tepe, N.; Doerr, S. H.; Hofmann, T. Environmentally persistent free radicals are ubiquitous in wildfire charcoals and remain stable for years. *Commun. Earth Environ.* **2021**, *2*, 68.
(24) Zhu, K. C.; Jia, H. Z.; Sun, Y. J.; Dai, Y. C.; Zhang, C.; Guo, X. T.; Wang, T. C.; Zhu, L. Y. Long-term phototransformation of microplastics under simulated sunlight irradiation in aquatic environments: Roles of reactive oxygen species. *Water Res.* **2020**, *173*, No. 115564.
(25) Liu, Z.; Sun, Y. J.; Wang, J. Q.; Li, J. H.; Jia, H. Z. In vitro assessment reveals the effects of environmentally persistent free radicals on the toxicity of photoaged tire wear particles. *Environ. Sci. Technol.* **2022**, *56*, 1664−1674.
(26) Sarkar, B.; Mandal, S. Microbial Degradation of Natural and Synthetic Rubbers. In *Microbial Bioremediation & Biodegradation.*; Shah, M. P., Ed.; Springer: Singapore, 2020; pp 527−550.
(27) Altenhoff, A. L.; de Witt, J.; Andler, R.; Steinbuchel, A. Impact of additives of commercial rubber compounds on the microbial and enzymatic degradation of poly(cis-1,4-isoprene). *Biodegradation* **2019**, *30*, 13−26.
(28) Christiansson, M.; Stenberg, B.; Holst, O. Toxic additives-A problem for microbial waste rubber desulphurisation. *Resour. Environ. Biotechnol.* **2000**, *3*, 11−21.
(29) Wagner, S.; Klockner, P.; Reemtsma, T. Aging of tire and road wear particles in terrestrial and freshwater environments-A review on processes, testing, analysis and impact. *Chemosphere* **2022**, *288*, No. 132467.
(30) Kreider, M. L.; Panko, J. M.; McAtee, B. L.; Sweet, L. I.; Finley, B. L. Physical and chemical characterization of tire-related particles: Comparison of particles generated using different methodologies. *Sci. Total Environ.* **2010**, *408*, 652−659.
(31) Ding, J.; Meng, F. Y.; Chen, H.; Chen, Q. L.; Hu, A. Y.; Yu, C. P.; Chen, L. X.; Lv, M. Leachable additives of tire particles explain the shift in microbial community composition and function in coastal sediments. *Environ. Sci. Technol.* **2022**, *56*, 12257−12266.
(32) Han, R. X.; Lv, J. T.; Huang, Z. Q.; Zhang, S. H.; Zhang, S. Z. Pathway for the production of hydroxyl radicals during the microbially mediated redox transformation of iron (oxyhydr)oxides. *Environ. Sci. Technol.* **2020**, *54*, 902−910.
(33) Han, R. X.; Wang, Z.; Lv, J. T.; Zhu, Z.; Yu, G. H.; Li, G.; Zhu, Y. G. Multiple effects of humic components on microbially mediated iron redox processes and production of hydroxyl radicals. *Environ. Sci. Technol.* **2022**, *56*, 16419−16427.
(34) Sutherland, M. W.; Learmonth, B. The tetrazolium dyes MTS and XTT provide new quantitative assays for superoxide and superoxide dismutase. *Free Radical Res.* **1997**, *27*, 283−289.
(35) Li, B.-Q.; Zhao, C. X.; Liu, J. N.; Zhang, Q. Electrosynthesis of hydrogen peroxide synergistically catalyzed by atomic Co−Nx−C sites and oxygen functional groups in noble-metal-free electrocatalysts. *Adv. Mater.* **2019**, *31*, No. 1904044.
(36) Xie, W. J.; Yuan, S. H.; Tong, M.; Ma, S. C.; Liao, W. J.; Zhang, N.; Chen, C. M. Contaminant degradation by •OH during sediment oxygenation: dependence on Fe(II) species. *Environ. Sci. Technol.* **2020**, *54*, 2975−2984.
(37) Gehling, W.; Khachatryan, L.; Dellinger, B. Hydroxyl radical generation from environmentally persistent free radicals (EPFRs) in $PM_{2.5}$. *Environ. Sci. Technol.* **2014**, *48*, 4266−4272.
(38) Jia, H. Z.; Zhao, S.; Nulaji, G.; Tao, K. L.; Wang, F.; Sharma, V. K.; Wang, C. Y. Environmentally persistent free radicals in soils of past coking sites: Distribution and stabilization. *Environ. Sci. Technol.* **2017**, *51*, 6000−6008.
(39) Seiwert, B.; Nihemaiti, M.; Troussier, M.; Weyrauch, S.; Reemtsma, T. Abiotic oxidative transformation of 6-PPD and 6-PPD quinone from tires and occurrence of their products in snow from urban roads and in municipal wastewater. *Water Res.* **2022**, *212*, No. 118122.
(40) Huang, J. Z.; Jones, A.; Waite, T. D.; Chen, Y. L.; Huang, X. P.; Rosso, K. M.; Kappler, A.; Mansor, M.; Tratnyek, P. G.; Zhang, H. C. Fe(II) redox chemistry in the environment. *Chem. Rev.* **2021**, *121*, 8161−8233.
(41) Chen, S. S.; Yang, Y. T.; Jing, X. Y.; Zhang, L. L.; Chen, J.; Rensing, C.; Luan, T. G.; Zhou, S. G. Enhanced aging of polystyrene microplastics in sediments under alternating anoxic-oxic conditions. *Water Res.* **2021**, *207*, No. 117782.
(42) Stern, N.; Mejia, J.; He, S. M.; Yang, Y.; Ginder-Vogel, M.; Roden, E. E. Dual role of humic substances as electron donor and shuttle for dissimilatory iron reduction. *Environ. Sci. Technol.* **2018**, *52*, 5691−5699.
(43) Wu, X. W.; Liu, P.; Gong, Z. M.; Wang, H. Y.; Huang, H. X. Y.; Shi, Y. Q.; Zhao, X. L.; Gao, S. X. Humic acid and fulvic acid hinder long-term weathering of microplastics in lake water. *Environ. Sci. Technol.* **2021**, *55*, 15810−15820.
(44) Zhong, D. L.; Jiang, Y.; Zhao, Z. Z.; Wang, L. L.; Chen, J.; Ren, S. P.; Liu, Z. H.; Zhang, Y. R.; Tsang, D. C. W.; Crittenden, J. C. pH dependence of arsenic oxidation by rice-husk-derived biochar: roles of redox-active moieties. *Environ. Sci. Technol.* **2019**, *53*, 9034−9044.
(45) Ding, L.; Yu, X. Q.; Guo, X. T.; Zhang, Y. P.; Ouyang, Z. Z.; Liu, P.; Zhang, C.; Wang, T. C.; Jia, H. Z.; Zhu, L. Y. The photodegradation processes and mechanisms of polyvinyl chloride and polyethylene terephthalate microplastic in aquatic environments: Important role of clay minerals. *Water Res.* **2022**, *208*, No. 117879.
(46) Jia, H. Z.; Nulaji, G.; Gao, H. W.; Wang, F.; Zhu, Y. Q.; Wang, C. Y. Formation and stabilization of environmentally persistent free radicals induced by the interaction of anthracene with Fe(III)-modified clays. *Environ. Sci. Technol.* **2016**, *50*, 6310−6319.
(47) Zhu, K. C.; Jia, H. Z.; Zhao, S.; Xia, T. J.; Guo, X. T.; Wang, T. C.; Zhu, L. Y. Formation of environmentally persistent free radicals on microplastics under light irradiation. *Environ. Sci. Technol.* **2019**, *53*, 8177−8186.
(48) Ruan, X. X.; Sun, Y. Q.; Du, W. M.; Tang, Y. Y.; Liu, Q.; Zhang, Z. Y.; Doherty, W.; Frost, R. L.; Qian, G. R.; Tsang, D. C. W. Formation, characteristics, and applications of environmentally persistent free radicals in biochars: A review. *Bioresour. Technol.* **2019**, *281*, 457−468.

https://doi.org/10.1021/acs.est.2c08672
Environ. Sci. Technol. XXXX, XXX, XXX−XXX

(49) Pan, B.; Li, H.; Lang, D.; Xing, B. S. Environmentally persistent free radicals: Occurrence, formation mechanisms and implications. *Environ. Pollut.* **2019**, *248*, 320−331.
(50) Qin, Y.; Zhang, L.; An, T. Hydrothermal carbon-mediated Fenton-like reaction mechanism in the degradation of alachlor: Direct electron transfer from hydrothermal carbon to Fe(III). *ACS Appl. Mater. Interfaces* **2017**, *9*, 17115−17124.

https://doi.org/10.1021/acs.est.2c08672
Environ. Sci. Technol. XXXX, XXX, XXX−XXX